

UC Irvine

UC Irvine Previously Published Works

Title

Evaluation of Regional Climate Models Using Regionally Optimized GRACE Mascons in the Amery and Getz Ice Shelves Basins, Antarctica

Permalink

<https://escholarship.org/uc/item/7sm4f4qt>

Journal

Geophysical Research Letters, 46(23)

ISSN

0094-8276

Authors

Mohajerani, Yara
Velicogna, Isabella
Rignot, Eric

Publication Date

2019-12-16

DOI

10.1029/2019gl084665

Copyright Information

This work is made available under the terms of a Creative Commons Attribution License, available at <https://creativecommons.org/licenses/by/4.0/>

Peer reviewed

1 **Evaluation of Regional Climate Models using**
2 **Regionally-Optimized GRACE Mascons in the Amery**
3 **and Getz ice shelves basins, Antarctica**

4 **Yara Mohajerani¹, Isabella Velicogna^{1,2}, Eric Rignot^{1,2}**

5 ¹University of California, Earth System Science, Irvine, CA 92617, USA

6 ²Jet Propulsion Laboratory, CA 91109, USA

7 **Key Points:**

- 8 • The drainage of Getz Ice Shelf, West Antarctica is rapidly losing mass whereas
9 the drainage of Amery Ice Shelf is near balance.
- 10 • The GRACE mass balance agrees with the mass budget method with several re-
11 gional climate models on Getz but only with RACMO2.3p1 on Amery.
- 12 • The GRACE-based methodology helps evaluate RCMs and increase confidence in
13 mass balance estimates around Antarctica.

Corresponding author: Yara Mohajerani, ymohajer@uci.edu

This article has been accepted for publication and undergone full peer review but has not been through the copyediting, typesetting, pagination and proofreading process, which may lead to differences between this version and the Version of Record. Please cite this article as doi: 10.1029/2019GL084665

Abstract

We develop regionally-optimized GRACE solutions to evaluate the mass balance of the drainage basins of Amery Ice Shelf, East Antarctica and Getz Ice Shelf, West Antarctica. We find that the Amery region is near-balance, while the Getz region is rapidly losing mass. We compare the results with the Mass Budget Method (MBM) combining ice discharge along the periphery with surface mass balance derived from three regional climate models: 1) Regional Atmospheric Climate Model (RACMO) 2.3p1 and 2) 2.3p2, and 3) Modèle Atmosphérique Régional 3.6.41. For Amery, MBM/RACMO2.3p1 agrees with GRACE while MBM/RACMO2.3p2 and MBM/MAR3.6.41 suggest a positive mass balance. For Getz, all estimates agree with a mass loss and the GRACE results are robust to uncertainties in Glacial Isostatic Adjustment (GIA) derived from an ensemble of 128,000 forward models. Over the period 04/2002-11/2015, the mass loss of the Getz drainage basin is 22.9 ± 10.9 Gt/yr with an acceleration of 1.6 ± 0.9 Gt/yr².

Plain Language Summary

We use a regional optimization methodology for processing data from the Gravity Recovery and Climate Experiment (GRACE) to evaluate the ice mass change of the drainage basins of two major ice shelves in Antarctica and evaluate the performance of Regional Climate Models (RCMs). The Getz Ice Shelf basin in West Antarctica has shown previous disagreements between various mass balance estimates and is influenced by heterogeneous conditions that make it vulnerable and challenging to study. We find this region to be in a state of accelerating mass loss. Furthermore, all three examined RCMs are in good agreement with GRACE in this region. The Amery Ice Shelf in East Antarctica is the third largest Antarctic ice shelf with a basin that has enough ice to raise sea level by 7.8 meters, but has presented challenges in previous mass balance efforts. We find the mass in this drainage basin is not changing significantly. Furthermore, only one out of the three examined RCMs agrees with GRACE observations in this region. These results suggest that the RCMs may need to be revisited in some regions of the ice sheet.

1 Introduction

The Antarctic ice sheet has been losing mass at an average rate of 109 ± 56 Gt/yr from 1992 to 2017, equivalent to 7.6 ± 3.9 mm of sea level rise (Shepherd et al., 2018). During that time period, the mass loss has been accelerating (Velicogna et al., 2014; Rig-

not et al., 2019). The evaluation of ice sheet mass balance has been primarily achieved using a combination of three techniques: 1. gravimetric estimates from the GRACE (Gravity Recovery and Climate Experiment) mission (Velicogna et al., 2014; Sasgen et al., 2013; Velicogna & Wahr, 2006); 2. volume changes estimated from a series of altimeter measurements (Pritchard et al., 2012; McMillan et al., 2014; Sutterley et al., 2018); and 3. Mass Budget Method (MBM) combining ice discharge along the periphery with Surface Mass Balance (SMB) reconstructed by regional climate models (RCMs) in the interior (Rignot et al., 2008, 2019). While there is reasonable agreement between these large-scale estimates in West Antarctica (Shepherd et al., 2018, 2012), differences exist in East Antarctica. For instance, Shepherd et al. (2018) finds a standard deviation of 37 Gt/yr across the various mass balance estimates for East Antarctica. Moreover, regional differences between mass balance estimates have not been fully evaluated around Antarctica. Differences in RCMs affect not only the confidence on mass budget and altimetry estimates, with the latter due to firn compaction models forced by RCMs (Shepherd et al., 2012), but also impact the estimation of the partitioning in mass loss between SMB processes and ice dynamics for all techniques.

In a prior study, Mohajerani et al. (2018) used a regional optimization approach for GRACE to calculate the mass balance of Totten and Moscow University glaciers at the basin and sub-basin scales and evaluate different RCMs. Here, we extend the methodology to two major drainage systems in Antarctica. First, we examine the drainage basin feeding into the Amery Ice Shelf, which includes three major glaciers: Fisher, Lambert, Mellor, and two large sectors on the flanks of Amery Ice Shelf: MacRobertson Land and American HighLand. Amery is the third largest ice shelf in area in Antarctica (Pittard et al., 2017). Here we are interested in the mass balance of the drainage basin of the Amery Ice Shelf, which holds enough ice to raise sea level by 7.8 m (Rignot et al., 2019). At present, the basin appears to be in balance based on the mass budget method (Rignot et al., 2019). This region has presented challenges in past studies caused by differences in the estimation of the position of the grounding line. While some studies place it north of the 35 km Minimum Ice Shelf Width (MISW) (Winkelmann et al., 2012; Gолledge et al., 2015), others placing it to the south (DeConto & Pollard, 2016). Such differences result in major uncertainties in the mass balance of the Amery drainage basin.

Second is the drainage basin of the Getz Ice Shelf, which, according to the MBM, tripled its mass loss in 2017 compared to the 1979-2013 average, from 5 Gt/yr to 16.5

78 Gt/yr, for a cumulative contribution of 1mm to sea level rise from 1979 to 2017 (Rignot
79 et al., 2019). Most of the glaciers feeding into Getz Ice Shelf have no name and are la-
80 beled using a latitude-longitude convention (Rignot et al., 2019). The ice shelf, which
81 has a strong effect on the mass balance of the drainage basin due to its buttressing ef-
82 fect (Dupont & Alley, 2005), is located at a critical position in the Pacific-Antarctic coast-
83 line and strongly affected by decadal Pacific Oscillations (Jacobs et al., 2013). Spatial
84 heterogeneity due to different oceanic regimes to the west and east of the ice self, as well
85 as the complex bathymetry of the region make the analysis of the ice shelf evolution dif-
86 ficult (Jacobs et al., 2013), which in turns introduces uncertainty in the long-term mass
87 balance of the drainage basin. In addition, previous assessments of the mass balance of
88 the drainage basin have suggested major disagreements between GRACE and MBM es-
89 timates. For example, Sasgen et al. (2010) found that the GRACE estimate for the Getz
90 Ice Shelf and Pine Island Glacier basins were 26 Gt/yr lower than the MBM estimate.
91 This discrepancy could not be accounted for by the choice of the Glacial Isostatic Ad-
92 justment (GIA), or leakage from the atmosphere, ocean, or changes in other basins. The
93 authors attributed it to an anomalous mass gain that took place during the GRACE pe-
94 riod (August 2002 - August 2008) that was not included in their MBM estimate from
95 1980-2004, or possible errors in ice thickness along the grounding line. More recently,
96 Chuter et al. (2017) used ice thickness values derived from Cryosat-2 to reassess the mass
97 budget of Getz and deduced a near mass balance of 5 ± 17 Gt/yr for 2006 to 2008. This
98 estimate is within one standard deviation of prior radar altimetry estimates (Shepherd
99 et al., 2012) but far more positive than prior estimates. The authors attributed this dif-
100 ference to a 9 m positive bias in elevation near the grounding line in the ERS-1 digital
101 elevation model (Griggs & Bamber, 2011). The most recent MBM estimates from this
102 area are however based on actual thickness data, not on hydrostatic equilibrium (Rignot
103 et al., 2019). In this study, we compare the mass balance estimates from GRACE and
104 MBM using various RCMs to establish a greater level of confidence in the results, eval-
105 uate different RCMs, and resolve uncertainties from prior studies. We conclude on the
106 mass loss of these major sectors and on the evaluation of RCMs.

107 **2 Data and Methodology**

108 We use three RCMs: 1) Regional Atmospheric Climate Model version 2.3p1 (RACMO2.3p1)
109 (Van Wessem et al., 2014), 2) version 2.3p2 (RACMO2.3p2) (van Wessem et al., 2018),

110 and 3) Modèle Atmosphérique Régional version 3.6.41 (MAR3.6.41) (Agosta et al., 2019).
111 RACMO2, developed by the Institute for Marine and Atmospheric Research Utrecht (IMAU)
112 at Utrecht University, uses the physics package of the Integrated Forecast System (IFS)
113 of the European Centre for Medium-Range Weather Forecasts (ECMWF) along with the
114 HIRLAM (High Resolution Limited Area Model) (Undén et al., 2002) dynamics to model
115 SMB (Van Wessem et al., 2014) at 27km resolution. RACMO2.3p2 provides several up-
116 dates to part 1, including improved topography, precipitation, and snow properties (van
117 Wessem et al., 2018). RACMO2.3p1 is available from 1979 to 2015. RACMO2.3p2 is avail-
118 able from 1979 to 2016. MAR3.6.41 is a coupled surface-atmosphere regional climate model
119 that uses the SISVAT surface scheme (Soil Ice Snow Vegetation Atmosphere Transfer)
120 (De Ridder & Gallée, 1998), which uses the CROCUS snow model (Brun et al., 1992).
121 The model estimates SMB at a spatial resolution of 35km for 1979 to 2017 (Agosta et
122 al., 2019). We use the version of the model forced by the ECMWF ERA-Interim reanal-
123 ysis (Dee et al., 2011) at the boundary to be consistent with RACMO2 (Agosta et al.,
124 2019; Van Wessem et al., 2014). While the choice of the forcing reanalysis product in-
125 troduces additional uncertainty, here we are interested in how the RCM parameteriza-
126 tions and processes diverge under the same forcing at the boundary.

127 To calculate MBM with each RCM, we interpolate the SMB fields to a $1\text{km}\times 1\text{km}$
128 polar stereographic grid and integrate the monthly values within each basin. Ice discharge
129 is from Rignot et al. (2019) with the following errors: 3.6 Gt/yr for Amery and 4.8 Gt/yr
130 for Getz. The regional SMB uncertainty is also from Rignot et al. (2019). The SMB and
131 discharge time-series are added up cumulatively, and the difference of the cumulative time-
132 series provides the total mass budget. By subtracting total cumulative discharge from
133 SMB, we eliminate the reliance on calculating anomalies with respect to a chosen ref-
134 erence period, i.e. the calculation of total mass budget numbers does not depend on the
135 choice of a reference period. Only the SMB and discharge anomalies depend on a ref-
136 erence period, not the total mass budget. Finally, a rate-of-change time-series is calcu-
137 lated by using a 36-month sliding window as described in the Supporting Information.

138 For each region, we get gravimetric estimates from GRACE (Tapley et al., 2004)
139 for 2002 to 2017. We use RL06 Level-2 spherical harmonic coefficients from the Center
140 for Space Research (CSR) at the University of Texas (Bettadpur, 2018) for the period
141 April 2002 to August 2016. The $C_{2,0}$ coefficients, representing the oblateness of the geoid,
142 are replaced with Satellite Laser Ranging coefficients (Cheng et al., 2013). Furthermore,

143 in order to recover degree-1 terms representing geocenter translations not measured by
144 GRACE in the gravitational frame of reference, we follow the methodology of the im-
145 proved geocenter solution by Sutterley and Velicogna (2019), using the same corrections
146 applied to the GRACE harmonics used in the spherical cap mascon calculation, outlined
147 below, for consistency. The Sutterley and Velicogna (2019) solution uses an iterative method
148 to calculate geocenter terms with the effects of self-attraction and loading. The Max-
149 Planck-Institute for Meteorology Ocean Model (MPIOM) (Jungclauss et al., 2013) har-
150 monics provided as part of the RL06 data release are used in combination with the GRACE
151 mass change coefficients on land to iteratively solve for geocenter terms. The GRACE
152 coefficients are de-striped following Swenson and Wahr (2006), smoothed with a 300-km
153 radius Gaussian smoothing kernel (Wahr et al., 1998), and corrected with the A et al.
154 (2013) GIA model for the geocenter calculation.

155 To ensure that our results are robust with respect to the GIA correction, we use
156 the GIA statistics provided by Caron et al. (2018), which uses regional constraints and
157 variations of ice history and earth structure through 128,000 forward modeling runs to
158 provide a probability distribution function from which the expectation value of present-
159 day GIA and the full covariance matrix associated with the errors are derived. Using a
160 probability distribution function as opposed to a single GIA product allows us to assess
161 the robustness of our results with regards to the GIA correction. We assess the GIA er-
162 ror using the full covariance matrix following Wahr et al. (2006). The GIA probability
163 distribution samples a wide range of upper and lower mantle viscosities, lithosphere thick-
164 nesses, and ice history through separate scaling factors for Antarctic, Greenland, Lau-
165 rentide, Cordilleran, and Fennoscandian ice sheets. The resulting covariance matrix from
166 the Bayesian treatment of the ensemble of forward models provides larger uncertainty
167 bounds than previous reports (Caron et al., 2018), allowing a conservative estimate of
168 the role of GIA in the GRACE estimate.

169 To produce regionally-optimized estimates of mass balance from Level-2 GRACE
170 harmonics we use the least-squares mascon approach, which uses variable-sized spher-
171 ical caps described in Mohajerani et al. (2018). This procedure generates a set of region-
172 ally configured spherical caps based on the characteristics of the local mass change to
173 calculate localized mass balance estimates from the GRACE harmonics. The caps are
174 organized to sample roughly uniform distributions of mass. The design allows the sum
175 of the designated mascons to capture the mass change only within the area of interest

176 with minimal leakage from outside regions that exhibit significant mass change. A smaller
177 size allows each cap to sample a more uniform region and refine the spatial extent of the
178 area being sampled. However, smaller caps are more heavily influenced by noisier higher
179 degree (shorter wavelength) harmonics (Wahr et al., 2006). Therefore, a higher mass change
180 signal in the area of interest allows the use of slightly smaller caps without being dom-
181 inated by noise. GRACE Stokes coefficients are regressed against these regionally defined
182 spherical caps with uniform and unitary mass using a simultaneous least-squares fit to
183 calculate weights for each mascon (Jacob et al., 2012; Velicogna et al., 2014; Sutterley
184 et al., 2014). For the areas of interest, multi-layer hexagonal grids with different reso-
185 lutions are used to create the spherical caps. In the Amery region, the caps range from
186 2.7° to 3.2° in diameter. Our study area focuses on the sub-basin region spanning the
187 Fisher, Lambert, Mellor, American HighLand, and MacRobertson Land basins. The basins
188 are defined according to (Rignot et al., 2019). The sampled area is shown by caps 1,5,7
189 in the inset of Figure 1a. In the Getz region, the diameters range from 2.6° to 3.0° . Our
190 study region is the drainage basin of the Getz Ice Shelf, and also covers some of the smaller
191 neighboring regions of Hull, Land, Frostman, Lord, Shuman, Anandakrishnan, and Jackson-
192 Perkins. The sampled area is shown by caps 1 and 2 in the inset of Figure 1b. The SMB
193 under the kernel from these regions and the corresponding grounding line discharge are
194 also included in our MBM estimate for the Getz region. The total discharge error for the
195 region is 4.9 Gt/yr by adding regional errors from Rignot et al. (2019) in quadrature.

196 The sensitivity kernel of the mascon configuration (Jacob et al., 2012) shows that
197 the signal is being captured by the mascons of interest in each configuration (Figure 1).
198 Ideally, the kernel should have a value of 1 over the regions of interest and 0 elsewhere.
199 The configurations focus on the areas of high ice velocity within each basin, or highest
200 mass loss, with minimal uncertainty. In each region, the sensitivity kernel captures the
201 areas of highest change and has minimal leakage elsewhere. Furthermore, by showing where
202 the signal is being sampled, the kernel in Figure 1 illustrates that there are no effects
203 from the small gaps between the spherical caps due to the tails of the truncated harmon-
204 ics extending beyond the exact boundaries of the caps (Swenson & Wahr, 2002). While
205 most of the ringing is diverted to the ocean where the mass change signal is smaller, there
206 are small variations of the kernel around the zero contour throughout the ice sheet, yet
207 both the land/ocean leakage and the leakage from other basins are fully quantified, as
208 outlined below.

209 The land/ocean leakage is calculated in two ways. First, the sea level fingerprint
210 of the region of interest (Hsu & Velicogna, 2017) is scaled by the total mass change de-
211 rived from GRACE. This calculation produces an estimate of the contribution from land
212 to ocean, which is used to adjust the mass loss trend. We assume a conservative error
213 of 100% in the error budget for this correction. In addition, we take into account the con-
214 tribution of the ocean signal that leaks into the mascons of interest. While the sensitiv-
215 ity kernels in Figure 1 have ringing over the ocean, the atmospheric and oceanic com-
216 ponents are removed from the GRACE GSM harmonics and therefore there is minimal
217 signal in these areas. As a conservative estimate, we use the total ocean signal provided
218 by the GRACE ocean (GAD) harmonics, which correspond to the MPIOM ocean model
219 (Jungclauss et al., 2013) to calculate the ocean leakage error. This is accomplished by fit-
220 ting the GAD coefficients to the mascons of interest and calculating the trend and ac-
221 celeration of this leakage signal. The mascon-to-mascon leakage on the ice sheet is taken
222 into account in the error budget. We use a synthetic mass budget field derived from mod-
223 eled SMB and linearly-distributed dynamic loss as a function of ice thickness and speed
224 following Rignot et al. (2011). The synthetic field is divided up between the spherical
225 caps for each configuration and converted to harmonics. The leakage is calculated by fit-
226 ting the synthetic harmonics derived from each spherical cap to the mascons and quan-
227 tifying the recovered signal for each cap. The leakage is calculated using two distinct mea-
228 sures: 1) “island leakage”, which refers to how much signal leaks *outward* from a mas-
229 con of interest to other mascons, and 2) “hole leakage”, which refers to how much sig-
230 nal leaks *inward* from other regions to the mascon of interest. This is similar to the leak-
231 age calculation in Mohajerani et al. (2018) with a few important updates: instead of tak-
232 ing the maximum value between the “island” and “hole” leakages as the total leakage,
233 we calculate the difference between the two. This approach produces a better assessment
234 of the overall effect of leakage in the regions of interest. While taking the differences re-
235 duces the leakage value in some cases, it may also increase it if the two leakage solutions
236 have opposite signs. The other change in the leakage calculation is to use an updated
237 synthetic field with discharge values from Rignot et al. (2019) and RACMO2.3 p1 and
238 p2 SMB values. The total mass budget synthetic field is calculated by spreading the to-
239 tal discharge value in each basin as a function of the flux density calculated from ice speed
240 and ice thickness. The ice speed is obtained from the MEaSUREs ice velocity data (Rignot
241 et al., 2017) and ice thickness is from Bedmap2 (Fretwell et al., 2013). We use the to-

242 tal mass budget as the synthetic field instead of taking the maximum leakage obtained
243 from SMB-only and MBM fields, which provides a more accurate leakage estimate with
244 a more realistic synthetic field.

245 The interpolated SMB values are integrated within the kernel to produce analo-
246 gous estimates to the GRACE measurements. We use a threshold of 5% in how much
247 signal is captured by the kernel to construct polygons around the regions of interest for
248 the integration. In other words, anything that is captured by GRACE at the 0.95 level
249 will be present in the MBM integration. This threshold reduces the effect of small fluc-
250 tuations near zero in the kernel field. However, because the mascons are designed around
251 the areas of high mass change, the low values of the kernel are in regions of smaller change
252 and thus the value of the threshold does not have a significant impact on the results.

253 **3 Results**

254 Figure 1 shows the time-series of mass change, dM/dt , of the regionally-optimized
255 GRACE solutions and the corresponding mascon configuration and sensitivity kernels,
256 and the MBM time-series derived from RACMO2.3p1, RACMO2.3p2, and MAR3.6.41
257 for Amery and Getz. The GRACE trend errors are calculated using the leakage, regres-
258 sion, GIA, and ocean leakage errors as described in the previous section. The correspond-
259 ing errors for the MBM time-series are calculated from the regression error combined with
260 the SMB and discharge errors outlined in the previous section. The full breakdown of
261 the trend errors is in Table 1. For each region, we calculate a trend and acceleration ac-
262 cording to the Bayesian Information Criterion (BIC) (Burnham & Anderson, 2004). For
263 Amery, the GRACE estimate indicates near balance, with a linear trend of 1.8 ± 5.0 Gt/yr.
264 The MBM estimate using RACMO2.3p1 agrees with the GRACE estimate within -0.4 ± 2.7
265 Gt/yr. While the GRACE and MBM/RACMO2.3p1 estimates are statistically in near-
266 balance, the MBM/RACMO2.3p2 and MBM/MAR3.6.41 exhibit statistically significant
267 positive trends. Table 1 lists all trends for the common period of April 2002 to Novem-
268 ber 2015.

269 In contrast to Amery, none of the RCMs show a bias with respect to GRACE in
270 the Getz region. As shown in panel (b) of Figure 1, the GRACE and MBM time-series
271 are in excellent agreement. As outlined in Table 1 the GRACE estimate yields a loss of
272 22.9 ± 10.9 Gt/yr. The GRACE errors are larger in this area as a result of a larger leak-

273 age error. The leakage error poses a special challenge in this small sub-basin region given
274 that it is adjacent to the highest mass loss of the entire ice sheet recorded in the Amund-
275 sen Sea Embayment sector of West Antarctica (Velicogna et al., 2014). The correspond-
276 ing MBM mass loss estimates are 23.7 ± 6.2 Gt/yr, 23.8 ± 6.3 Gt/yr, and 25.4 ± 6.3 Gt/yr
277 for MAR3.6.41, RACMO2.3p1, and RACMO2.3p2 models, respectively, which are in ex-
278 cellent agreement with GRACE. The close agreement between estimates provide con-
279 fidence in the mass balance assessment using these independent methods. This area also
280 exhibits an acceleration in mass loss. Table 1 outlines the acceleration and correspond-
281 ing error for regions where a quadratic regression model is applicable. This is analogous
282 to Table 1, excluding the GIA errors, which do not affect the acceleration since the GIA
283 correction is a constant signal. We find an acceleration in mass loss of 1.6 ± 0.9 Gt/yr²
284 with GRACE, in agreement with the acceleration of 2.0 ± 0.2 Gt/yr² from MBM.

285 4 Discussion

286 Our regionally-optimized GRACE estimates indicate that the Amery region is near
287 balance, which confirms Rignot et al. (2019) using the MBM/RACMO2.3p1. This is also
288 in agreement with previous in-situ measurements. Wen et al. (2007) used a combination
289 of remote-sensing and in-situ data to find a near-balance mass budget of -2.6 ± 6.5 Gt/yr
290 for Lambert, Mellor, and Fisher glaciers. Similarly, Wen et al. (2014) found these glaciers
291 to be in balance within 2.9 ± 3.6 Gt/yr by combining SMB from RACMO2.1 with dis-
292 charge derived from interferometric synthetic-aperture radar (InSAR)-derived ice veloc-
293 ity and BEDMAP (Lythe & Vaughan, 2001) and PCMEGA (Prince Charles Mountains
294 Expedition of Germany and Australia) (Damm, 2007) derived ice thickness, which is in
295 agreement with MBM/RACMO2.3p1. In contrast, Yu et al. (2010) found a significantly
296 more positive trend of 22.9 ± 4.4 Gt/yr for the grounded portion of the Amery Ice Shelf
297 system by utilizing ICESat and InSAR with a refined grounding line position derived
298 from SAR and MODIS data. However, our findings suggest that this result overestimates
299 mass gain in the region, which may reflect the quality of the SMB model in Vaughan et
300 al. (1999). The RACMO model used by Wen et al. (2014) has lower accumulation lev-
301 els in the Lambert region compared to that in Vaughan et al. (1999).

302 In the Getz area, GRACE yields a mass loss of 22.9 ± 10.9 Gt/yr and acceleration
303 of 1.6 ± 0.9 Gt/yr², within errors of the mass loss of 16.5 Gt/yr in 2017 from Rignot et
304 al. (2019). Our estimate agrees with radar altimetry results from McMillan et al. (2014)

305 (22±3Gt/yr for 2010-2013) and GRACE from King et al. (2012) (23±3Gt/yr for the larger
306 drainage basin in 2002-2010). Previous MBM estimates using ice thickness from Cryosat-
307 2 (Chuter et al., 2017) however yielded a positive trend of 5±17Gt/yr, which does not
308 agree with GRACE despite the large uncertainty bound. Our MBM trends, all in ex-
309 cellent agreement with GRACE, do not confirm this positive estimate, which implies that
310 the Cryosat-2 derived thicknesses were probably too low, which is probably a result of
311 uncertainties in firn depth correction. Similarly, the gravimetric estimate of Bouman et
312 al. (2014) yields a significantly larger loss of 55±9 Gt/yr from November 2009 to June
313 2012 by combining GRACE with GOCE (Gravity Field and Steady-State Ocean Circu-
314 lation Explorer) (Visser et al., 2002). The agreement between our independent GRACE
315 and MBM estimates suggest that this earlier estimate of the mass loss is too high. Fur-
316 thermore, with the regionally-optimized mascon approach, we successfully isolated the
317 mass balance of the Getz drainage basin with a mascon-to-mascon leakage error that is
318 only 45% of the total signal (Table 1). Considering the proximity of this region to the
319 high mass change signal of Amundsen Sea Sector glaciers, we conclude that this demon-
320 strates the practicality of our approach at the sub-basin scale in Antarctica.

321 In the Amery region, we find that MBM/RACMO2.3p1 is in agreement with GRACE,
322 while MBM/RACMO2.3p2 and MBM/MAR3.6.41 produce trends that are too positive.
323 This result is consistent with those of Mohajerani et al. (2018) on Totten and Moscow
324 University glaciers in East Antarctica (Figure S1). Given that all mass budget estimates
325 in a given region share the same discharge values, the differences must be attributed to
326 the SMB models. As outlined in Section 2, the cumulative time-series are calculated by
327 integrating the total monthly SMB and discharge values through time. As a result, dif-
328 ferent trends in the MBM time-series must be attributed to either disagreeing tempo-
329 ral variability or differences in mean SMB across models. The monthly SMB time-series
330 do not exhibit statistically significant trends in any of the regions. However, there are
331 considerable differences in the mean magnitude of monthly SMB time-series, as outlined
332 in Table S1 Larger monthly magnitudes lead to faster cumulative growth compared to
333 the cumulative discharge time-series, resulting in a more positive MBM time-series. It
334 is important to emphasize that this result does not depend on a reference period since
335 the mass balance is simply the difference between absolute SMB and absolute discharge.

336 In the Amery region, where MBM/RACMO2.3p2 and MBM/MAR3.6.41 do not
337 agree with GRACE, the mean SMB values appear to be more than 10 Gt/yr larger com-

338 compared to RACMO2.3p1, yielding a more positive MBM trend consistent with Table 1.
339 In the Getz area, the mean SMB values are in better agreement across all models, con-
340 sistent with the agreement between MBM estimates and GRACE in Figure 1 and Ta-
341 ble 1. Given that the monthly SMB time-series do not exhibit significant trends and the
342 discharge values are the same across the MBM estimates, we conclude that the differ-
343 ences in mean SMB account for most of the disagreement between various MBM esti-
344 mates. This conclusion enables us to perform a simple adjustment of the SMB time-series
345 with the ratio of mean magnitude of RACMO2.3p1 to that of each model during the ref-
346 erence period, given that MBM/RACMO2.3p1 has the best agreement with GRACE.
347 Figure S2 shows the adjusted time-series for Amery, where the mean SMB from RACMO2.3p2
348 and MAR3.6.41 are lowered by 87.9%, and 87.1% respectively.

349 The modifications brought to RACMO2.3 version p2 compared to p1 made the coast-
350 line of East Antarctica drier and the interior regions wetter. Our assessment suggests
351 that the model modifications may need to be revisited in light of our multi-sensor as-
352 sessment, at least in the regions examined herein. In contrast, the impact of the model
353 upgrade is negligible in the examined portions of West Antarctica, where the multi-sensor
354 results agree within errors. Importantly, our results increase confidence in the large mass
355 loss observed in the Getz Ice Shelf sector of West Antarctica and its acceleration in mass
356 loss. We posit that this sector is strongly affected by enhanced intrusion of warm CDW
357 on the continental shelf and beneath the ice shelf, which melts the ice shelf and glaciers,
358 allows the glacier grounding lines to retreat, speed up the ice flow, which contributes to
359 sea level rise. In contrast, the Amery region is far from the sources of warm CDW and
360 its unique geometry provides buttressing on three sides of the ice shelf. The drainage basin
361 appears to be in a state of mass balance.

362 5 Conclusions

363 We quantify the mass balance of the drainage basins of two major regions of Antarc-
364 tica, the Amery Ice Shelf in East Antarctica, and the Getz Ice Shelf in West Antarctica,
365 using regionally-optimized GRACE mascons with minimal leakage. We compare the GRACE
366 results with the Mass Budget Method (MBM) estimates using three different RCM out-
367 put products. The Amery basin is in a state of mass balance, in agreement with MBM/RACMO2.3p1,
368 but not with higher previous estimates of Yu et al. (2010). Furthermore, we find MBM/RACMO2.3p2
369 and MBM/MAR3.6.41 produce significant positive trends of 8.8 ± 2.9 and 9.4 ± 2.7 Gt/yr,

370 respectively. These differences are attributed to the magnitude of the mean monthly SMB
371 values. Over Getz, we report a significant mass loss of 22.9 ± 10.9 Gt/yr, in agreement
372 with all MBM estimates. These estimates do not confirm positive trends derived with
373 Cryosat-2 (Chuter et al., 2017) and more negative trends from other gravimetric results
374 (Bouman et al., 2014). The Getz region exhibits an accelerating loss at 1.6 ± 0.9 Gt/yr²,
375 hence contributing to sea level rise at an accelerated pace. Overall, the regionally-optimized
376 GRACE solutions provide an independent evaluation of the RCMs. Documenting and
377 understanding the sources of these differences provides valuable insights about model per-
378 formance that will subsequently help improve RCMs and remove residual uncertainties
379 in the mass budget of Antarctica.

380 Acknowledgments

381 This work was performed at the University of California Irvine and at the Caltech Jet
382 Propulsion Laboratory under a contract with the National Aeronautics and Space Ad-
383 ministration Cryosphere Science Program. The Level-2 GRACE harmonics used in this
384 study can be accessed on the Physical Oceanography Distributed Active Archive Cen-
385 ter (PO.DAAC) at [https://podaac-tools.jpl.nasa.gov/drive/files/GeodeticsGravity/
386 grace/L2/CSR/RL06](https://podaac-tools.jpl.nasa.gov/drive/files/GeodeticsGravity/grace/L2/CSR/RL06). MAR surface mass balance is available at [ftp://ftp.climato.be/
387 fettweis/](ftp://ftp.climato.be/fettweis/). RACMO data is provided by the Institute for Marine and Atmospheric Re-
388 search (IMAU) at Utrecht University at [https://www.projects.science.uu.nl/iceclimate/
389 publications/data/2018/index.php](https://www.projects.science.uu.nl/iceclimate/publications/data/2018/index.php) and [https://doi.pangaea.de/10.1594/PANGAEA
390 .896940](https://doi.pangaea.de/10.1594/PANGAEA.896940). The data presented in this study is publicly accessible at [https://www.ess
391 .uci.edu/~velicogna/amery-getz.php](https://www.ess.uci.edu/~velicogna/amery-getz.php) and archived on Figshare according to the En-
392 abling FAIR data guidelines at <https://doi.org/10.6084/m9.figshare.9917210>.

393 References

- 394 A, G., Wahr, J., & Zhong, S. (2013). Computations of the viscoelastic response of a
395 3-d compressible earth to surface loading: an application to glacial isostatic ad-
396 justment in antarctica and canada. *Geophysical Journal International*, *192*(2),
397 557–572.
- 398 Agosta, C., Amory, C., Kittel, C., Orsi, A., Favier, V., Gallée, H., . . . others (2019).
399 Estimation of the antarctic surface mass balance using the regional cli-
400 mate model mar (1979–2015) and identification of dominant processes. *The*

401 *Cryosphere*, 13(1), 281–296.

402 Bettadpur, S. (2018). Gravity recovery and climate experiment utcsr level-2 process-
403 ing standards document for level-2 product release 0006. *University of Texas at*
404 *Austin, GRACE Doc, 327742*, 16.

405 Bouman, J., Fuchs, M., Ivins, E. v., Wal, W., Schrama, E., Visser, P., & Horwath,
406 M. (2014). Antarctic outlet glacier mass change resolved at basin scale from
407 satellite gravity gradiometry. *Geophysical Research Letters*, 41(16), 5919–
408 5926.

409 Brun, E., David, P., Sudul, M., & Brunot, G. (1992). A numerical model to sim-
410 ulate snow-cover stratigraphy for operational avalanche forecasting. *Journal of*
411 *Glaciology*, 38(128), 13–22.

412 Burnham, K. P., & Anderson, D. R. (2004). Multimodel inference: understand-
413 ing aic and bic in model selection. *Sociological methods & research*, 33(2), 261–
414 304.

415 Caron, L., Ivins, E., Larour, E., Adhikari, S., Nilsson, J., & Blewitt, G. (2018). Gia
416 model statistics for grace hydrology, cryosphere, and ocean science. *Geophys-
417 ical Research Letters*, 45(5), 2203–2212.

418 Cheng, M., Tapley, B. D., & Ries, J. C. (2013). Deceleration in the earth’s oblate-
419 ness. *Journal of Geophysical Research: Solid Earth*, 118(2), 740–747.

420 Chuter, S., Martín-Español, A., Wouters, B., & Bamber, J. L. (2017). Mass balance
421 reassessment of glaciers draining into the abbot and getz ice shelves of west
422 antarctica. *Geophysical Research Letters*, 44(14), 7328–7337.

423 Damm, V. (2007). A subglacial topographic model of the southern drainage area of
424 the lambert glacier/amery ice shelf system-results of an airborne ice thickness
425 survey south of the prince charles mountains. *Terra Antartica*, 14(1/2), 85.

426 DeConto, R. M., & Pollard, D. (2016). Contribution of antarctica to past and future
427 sea-level rise. *Nature*, 531(7596), 591.

428 Dee, D. P., Uppala, S., Simmons, A., Berrisford, P., Poli, P., Kobayashi, S., . . . oth-
429 ers (2011). The era-interim reanalysis: Configuration and performance of the
430 data assimilation system. *Quarterly Journal of the royal meteorological society*,
431 137(656), 553–597.

432 De Ridder, K., & Gallée, H. (1998). Land surface-induced regional climate change in
433 southern israel. *Journal of applied meteorology*, 37(11), 1470–1485.

- 434 Dupont, T., & Alley, R. B. (2005). Assessment of the importance of ice-shelf but-
435 tressing to ice-sheet flow. *Geophysical Research Letters*, *32*(4).
- 436 Fretwell, P., Pritchard, H. D., Vaughan, D. G., Bamber, J. L., Barrand, N., Bell, R.,
437 ... others (2013). Bedmap2: improved ice bed, surface and thickness datasets
438 for antarctica. *The Cryosphere*, *7*, 375–393.
- 439 Golledge, N. R., Kowalewski, D. E., Naish, T. R., Levy, R. H., Fogwill, C. J., &
440 Gasson, E. G. (2015). The multi-millennial antarctic commitment to future
441 sea-level rise. *Nature*, *526*(7573), 421.
- 442 Griggs, J. A., & Bamber, J. (2011). Antarctic ice-shelf thickness from satellite radar
443 altimetry. *Journal of Glaciology*, *57*(203), 485–498.
- 444 Hsu, C.-W., & Velicogna, I. (2017). Detection of sea level fingerprints derived from
445 grace gravity data. *Geophysical Research Letters*, *44*(17), 8953–8961.
- 446 Jacob, T., Wahr, J., Pfeffer, W. T., & Swenson, S. (2012). Recent contributions of
447 glaciers and ice caps to sea level rise. *Nature*, *482*(7386), 514–518.
- 448 Jacobs, S., Giulivi, C., Dutrieux, P., Rignot, E., Nitsche, F., & Mouginot, J. (2013).
449 Getz ice shelf melting response to changes in ocean forcing. *Journal of Geo-*
450 *physical Research: Oceans*, *118*(9), 4152–4168.
- 451 Jungelaus, J., Fischer, N., Haak, H., Lohmann, K., Marotzke, J., Matei, D., ...
452 Von Storch, J. (2013). Characteristics of the ocean simulations in the max
453 planck institute ocean model (mpiom) the ocean component of the mpi-earth
454 system model. *Journal of Advances in Modeling Earth Systems*, *5*(2), 422–
455 446.
- 456 King, M. A., Bingham, R. J., Moore, P., Whitehouse, P. L., Bentley, M. J., & Milne,
457 G. A. (2012). Lower satellite-gravimetry estimates of antarctic sea-level
458 contribution. *Nature*, *491*(7425), 586.
- 459 Lythe, M. B., & Vaughan, D. G. (2001). Bedmap: A new ice thickness and sub-
460 glacial topographic model of antarctica. *Journal of Geophysical Research: Solid*
461 *Earth*, *106*(B6), 11335–11351.
- 462 McMillan, M., Shepherd, A., Sundal, A., Briggs, K., Muir, A., Ridout, A., ... Wing-
463 ham, D. (2014). Increased ice losses from antarctica detected by cryosat-2.
464 *Geophysical Research Letters*, *41*(11), 3899–3905.
- 465 Mohajerani, Y., Velicogna, I., & Rignot, E. (2018). Mass loss of totten and moscow
466 university glaciers, east antarctica, using regionally optimized grace mascons.

467 *Geophysical Research Letters*, 45(14), 7010–7018.

468 Pittard, M., Galton-Fenzi, B., Watson, C., & Roberts, J. (2017). Future sea level
469 change from antarctica's lambert-amery glacial system. *Geophysical Research*
470 *Letters*, 44(14), 7347–7355.

471 Pritchard, H., Ligtenberg, S., Fricker, H., Vaughan, D., Van den Broeke, M., & Pad-
472 man, L. (2012). Antarctic ice-sheet loss driven by basal melting of ice shelves.
473 *Nature*, 484(7395), 502–505.

474 Rignot, E., Bamber, J. L., Van Den Broeke, M. R., Davis, C., Li, Y., Van De Berg,
475 W. J., & Van Meijgaard, E. (2008). Recent antarctic ice mass loss from
476 radar interferometry and regional climate modelling. *Nature geoscience*, 1(2),
477 106–110.

478 Rignot, E., Mouginot, J., & Scheuchl, B. (2011). Ice flow of the antarctic ice sheet.
479 *Science*, 333(6048), 1427–1430.

480 Rignot, E., Mouginot, J., & Scheuchl, B. (2017). *Measures insar-based antarctica ice*
481 *velocity map, version 2. boulder, colorado usa. nasa national snow and ice data*
482 *center distributed active archive center.*

483 Rignot, E., Mouginot, J., Scheuchl, B., van den Broeke, M., van Wessem, M. J.,
484 & Morlighem, M. (2019). Four decades of antarctic ice sheet mass balance
485 from 1979–2017. *Proceedings of the National Academy of Sciences*, 116(4),
486 1095–1103.

487 Sasgen, I., Konrad, H., Ivins, E., Van den Broeke, M., Bamber, J., Martinec, Z.,
488 & Klemann, V. (2013). Antarctic ice-mass balance 2003 to 2012: regional
489 reanalysis of grace satellite gravimetry measurements with improved estimate
490 of glacial-isostatic adjustment based on gps uplift rates. *The Cryosphere*, 7,
491 1499–1512.

492 Sasgen, I., Martinec, Z., & Bamber, J. (2010). Combined grace and insar estimate of
493 west antarctic ice mass loss. *Journal of Geophysical Research: Earth Surface*,
494 115(F4).

495 Shepherd, A., Ivins, E., Rignot, E., Smith, B., Van Den Broeke, M., Velicogna, I.,
496 ... others (2018). Mass balance of the antarctic ice sheet from 1992 to 2017.
497 *Nature*, 558, 219–222.

498 Shepherd, A., Ivins, E. R., Geruo, A., Barletta, V. R., Bentley, M. J., Bettadpur, S.,
499 ... others (2012). A reconciled estimate of ice-sheet mass balance. *Science*,

500 338(6111), 1183–1189.

501 Sutterley, T. C., & Velicogna, I. (2019). Improved estimates of geocenter variability
502 from time-variable gravity and ocean model outputs. *Remote Sensing*, 11(18),
503 2108.

504 Sutterley, T. C., Velicogna, I., Csatho, B., van den Broeke, M., Rezvan-Behbahani,
505 S., & Babonis, G. (2014). Evaluating greenland glacial isostatic adjustment
506 corrections using grace, altimetry and surface mass balance data. *Environment-
507 tal Research Letters*, 9(1), 014004.

508 Sutterley, T. C., Velicogna, I., Fettweis, X., Rignot, E., Noël, B., & van den Broeke,
509 M. (2018). Evaluation of reconstructions of snow/ice melt in greenland by
510 regional atmospheric climate models using laser altimetry data. *Geophysical
511 Research Letters*, 45(16), 8324–8333.

512 Swenson, S., & Wahr, J. (2002). Methods for inferring regional surface-mass anoma-
513 lies from gravity recovery and climate experiment (grace) measurements of
514 time-variable gravity. *Journal of Geophysical Research: Solid Earth*, 107(B9).

515 Swenson, S., & Wahr, J. (2006). Post-processing removal of correlated errors in
516 grace data. *Geophysical Research Letters*, 33(8).

517 Tapley, B. D., Bettadpur, S., Watkins, M., & Reigber, C. (2004). The gravity re-
518 covery and climate experiment: Mission overview and early results. *Geophys-
519 ical Research Letters*, 31(9).

520 Undén, P., Rontu, L., Jarvinen, H., Lynch, P., Calvo Sánchez, F. J., Cats, G., ...
521 others (2002). Hirlam-5 scientific documentation.

522 Van Wessem, J., Reijmer, C., Morlighem, M., Mouginot, J., Rignot, E., Medley, B.,
523 ... others (2014). Improved representation of east antarctic surface mass bal-
524 ance in a regional atmospheric climate model. *Journal of Glaciology*, 60(222),
525 761–770.

526 van Wessem, J. M., Jan Van De Berg, W., Noël, B. P., Van Meijgaard, E., Amory,
527 C., Birnbaum, G., ... others (2018). Modelling the climate and surface mass
528 balance of polar ice sheets using racmo2: Part 2: Antarctica (1979-2016).
529 *Cryosphere*, 12(4), 1479–1498.

530 Vaughan, D. G., Bamber, J. L., Giovinetto, M., Russell, J., & Cooper, A. P. R.
531 (1999). Reassessment of net surface mass balance in antarctica. *Journal of
532 climate*, 12(4), 933–946.

- 533 Velicogna, I., Sutterley, T., & van den Broeke, M. (2014). Regional acceleration in
534 ice mass loss from greenland and antarctica using grace time-variable gravity
535 data. *Geophysical Research Letters*, *41*(22), 8130–8137.
- 536 Velicogna, I., & Wahr, J. (2006). Measurements of time-variable gravity show mass
537 loss in antarctica. *science*, *311*(5768), 1754–1756.
- 538 Visser, P., Rummel, R., Balmino, G., Sünkel, H., Johannessen, J., Aguirre, M., ...
539 Sabadini, R. (2002). The european earth explorer mission goce: impact for the
540 geosciences. *Ice Sheets, Sea Level and the Dynamic Earth*, *29*, 95–107.
- 541 Wahr, J., Molenaar, M., & Bryan, F. (1998). Time variability of the earth's gravity
542 field: Hydrological and oceanic effects and their possible detection using grace.
543 *Journal of Geophysical Research: Solid Earth*, *103*(B12), 30205–30229.
- 544 Wahr, J., Swenson, S., & Velicogna, I. (2006). Accuracy of grace mass estimates.
545 *Geophysical Research Letters*, *33*(6).
- 546 Wen, J., Huang, L., Wang, W., Jacka, T., Damm, V., & Liu, Y. (2014). Ice thickness
547 over the southern limit of the amery ice shelf, east antarctica, and reassess-
548 ment of the mass balance of the central portion of the lambert glacier-amery
549 ice shelf system. *Annals of Glaciology*, *55*(66), 81–86.
- 550 Wen, J., Jezek, K. C., Csathó, B. M., Herzfeld, U. C., Farness, K. L., & Huybrechts,
551 P. (2007). Mass budgets of the lambert, mellor and fisher glaciers and basal
552 fluxes beneath their flowbands on amery ice shelf. *Science in China Series D:
553 Earth Sciences*, *50*(11), 1693–1706.
- 554 Winkelmann, R., Levermann, A., Martin, M. A., & Frieler, K. (2012). Increased fu-
555 ture ice discharge from antarctica owing to higher snowfall. *Nature*, *492*(7428),
556 239.
- 557 Yu, J., Liu, H., Jezek, K. C., Warner, R. C., & Wen, J. (2010). Analysis of veloc-
558 ity field, mass balance, and basal melt of the lambert glacier–amery ice shelf
559 system by incorporating radarsat sar interferometry and icesat laser altimetry
560 measurements. *Journal of Geophysical Research: Solid Earth*, *115*(B11).

Table 1. Trends and accelerations and associated errors for the Amery and Getz drainage basins, Antarctica, from April 2002 to November 2015 (shifted to mid-month values to match GRACE). For each drainage basin the results obtained from GRACE corrected with Caron et al. (2018) GIA model from the expectation of a probability distribution from 128,000 forward models, and the Mass Budget Method (MBM) estimates obtained from RACMO2.3p1, RACMO2.3p2, and MAR3.6.41 are shown. The leakage between mascons is estimated from a synthetic field, while the ocean leakage is obtained from the GRACE coefficients representing ocean-only changes (GAD coefficients).

	Trend / Acc.	Total Error	Leakage Error	Regression Error	Ocean Leakage	GIA Error
Trend[Gt/yr]						
<i>Amery</i>						
GRACE	1.77	5.04	2.36	1.55	-0.73	4.11
MBM/MAR3.6.41	9.45	2.72				
MBM/RACMO2.3p1	-0.39	2.65				
MBM/RACMO2.3p2	8.85	2.88				
<i>Getz</i>						
GRACE	-22.91	10.91	10.28	1.44	0.56	3.21
MBM/MAR3.6.41	-23.64	6.19				
MBM/RACMO2.3p1	-23.84	6.27				
MBM/RACMO2.3p2	-25.35	6.28				
Acceleration[Gt/yr^2]						
<i>Getz</i>						
GRACE	-1.57	0.88	0.25	0.82	0.04	–
MBM/MAR3.6.41	-1.56	0.21				
MBM/RACMO2.3p1	-2.01	0.19				
MBM/RACMO2.3p2	-1.77	0.24				

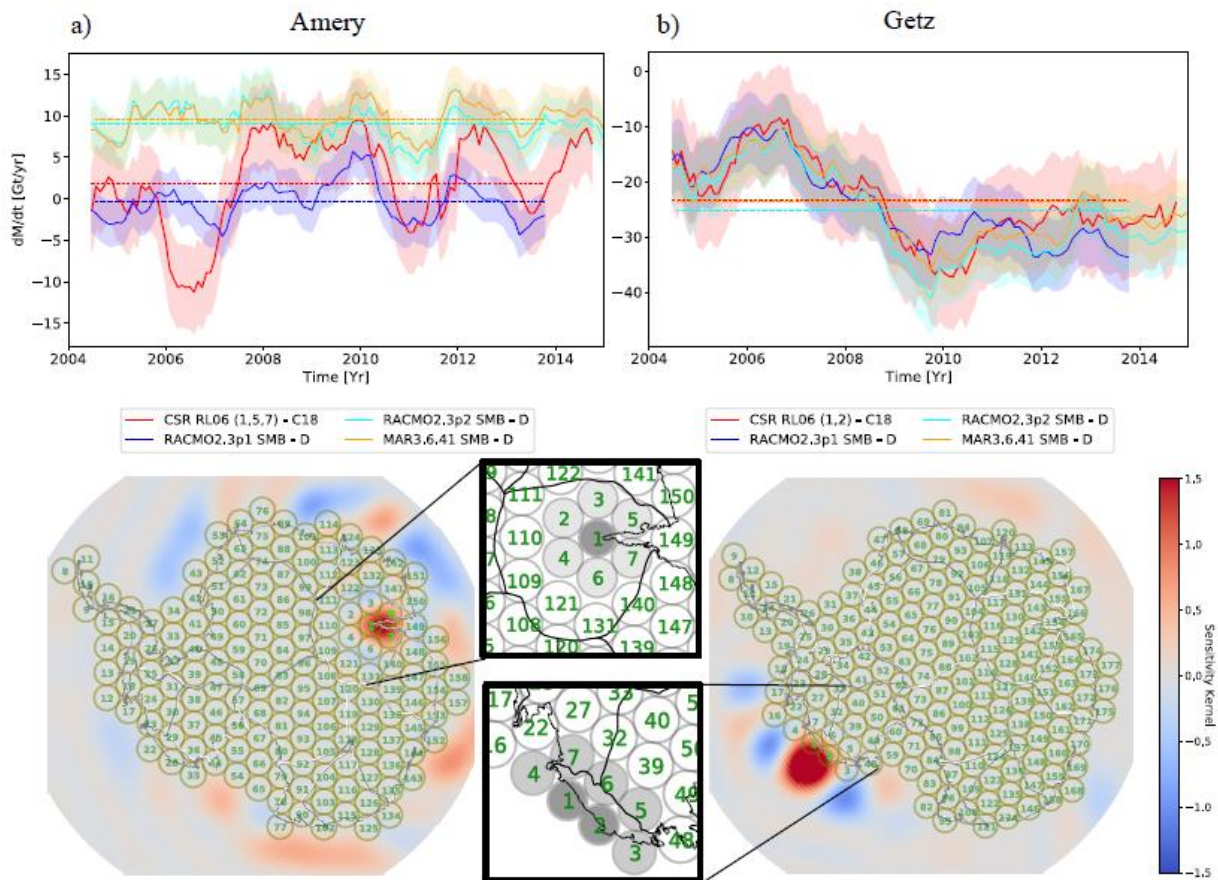


Figure 1. The rate of mass change time-series (dM/dt) in gigatons per year (10^{12} kg per year) obtained from a 36-month sliding window for (a) Amery and (b) Getz drainage basins, Antarctica, comparing the regionally optimized GRACE time-series (red) with the Mass Budget Method (MBM) estimate using RACMO2.3p1 (blue), RACMO2.3p2 (cyan), and MAR3.6.41 (orange). The dotted lines represent the mean trend during the common period. The corresponding mascon configurations and sensitivity kernels are shown below each time-series. The spherical caps are shown in gray circles, with the corresponding numerical labels in green. The caps used for the mass balance estimate are labelled in bright green. The insets show zoomed-in views of the caps of interest, with the lighter colors corresponding to increasing diameter — Amery: 2.7° (black), 2.9° (gray), and 3.2° (white); Getz: 2.6° (black), 2.8° (gray), and 3.0° (white).

A